
A G2(+) Level Investigation of the Gas-Phase Non-Identity S_N2 Reactions of Halides with Halodimethylamine

Yi Ren

Faculty of Chemistry, Sichuan University, Chengdu, People's Republic of China

Hua-jie Zhu

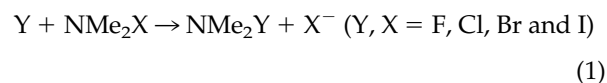
State Key Laboratory of Phytochemistry and Plant Resources in West China, CAS, Kunming, People's Republic of China

The gas-phase non-identity S_N2 reactions on nitrogen Y⁻ + NMe₂X → NMe₂Y + X⁻ (Y, X = F, Cl, Br, and I) were evaluated at the G2(+) level. The reactions are exothermic only when the nucleophile is the lighter halide. The complexation enthalpies for complexes Y⁻...Me₂NX are found to correlate with electronegativity of X. Both central and overall barriers can be interpreted with the aid of Marcus equation. Kinetic and thermodynamic investigations predict that the nucleophilicity of X⁻ decreases in the order: F⁻ > Cl⁻ > Br⁻ > I⁻ and the leaving-group ability increases in the order: F < Cl < Br < I. (J Am Soc Mass Spectrom 2004, 15, 673–680) © 2004 American Society for Mass Spectrometry

In the last decade, S_N2 reactions at formal neutral nitrogen have become the focus of interesting attention [1–9] because of their synthetic, biochemical and theoretical importance. Using double labeling experiments, Beak and Li [5] inferred the existence of a classical S_N2 transition state at a nitrogen substrate in the liquid phase. Theoretical studies of Bühl and Schaefer III [7] support the existence of conventional backside S_N2 transition state structures in reactions Y⁻ + NH₂X → NH₂Y + X⁻ (Y, X = F, Cl, OH, CN, H). Glukhovtsev et al. [8] reported G2(+) level calculation for the gas phase identity S_N2 reactions X⁻ + NH₂X → NH₂X + X⁻ (X = F–I). More recently, Gareyev et al. [6] studied the reactions of NH₂Cl with HO⁻, RO⁻(R = Me, Et, Pr, PhCH₂, CF₃CH₂), F⁻, HS⁻, and Cl⁻ in the gas phase using the selected ion flow tube technique and found that nucleophilic substitution at nitrogen to form Cl⁻ was observed for all the nucleophile and was faster than the corresponding reactions of methyl chloride. All of these studies revealed some similarities and differences between anionic S_N2 reactions at nitrogen and carbon.

We have recently reported [9] theoretical studies of some identity S_N2 reactions on nitrogen using G2(+) theory. The results led to the important conclusion that the Periodic Table, through the valence of the element X, controls the central barrier heights for the reactions H_nX⁻ + NMe₂XH_n (X = F, Cl, Br, I, O, S, Se, N, P, C),

similarly to the previously observed phenomenon for S_N2 reactions on carbon. We now extend our G2(+) study to non-identity reactions (eq 1). The present work represents the first uniform computational study of this fundamental reaction for all of the halogens at such a high level and will hopefully provide more reliable energy parameters. We also wish to apply the Marcus theory [10–12] to the displacement S_N2 reactions at nitrogen. Meanwhile, we will discuss the nucleophilicity of halide anion in gas-phase S_N2 reactions at nitrogen.

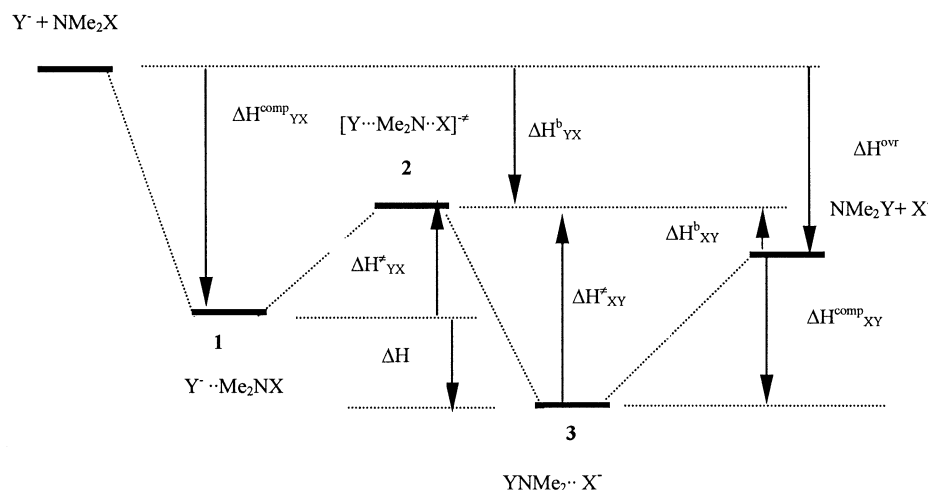


Methodology

The geometries of all species were fully optimized at the HF/6-31 + G(d) level first and re-optimized by MP2(fc)/6-31+ G(d). The nature of all optimized structure was determined using frequencies analysis at the HF/6-31 + G(d) level. A scaling factor of 0.8929 [13] was used for zero-point vibration energy (ZPVE) corrections in the calculations of relative enthalpies. All electron (AE) calculations were run for the fluorine- and chlorine-containing species, while Wadt and Hay [14] effective core potentials (ECP) were used for bromine- and iodine-containing species, referred as G2(+)–ECP. Full details of G2(+) procedure are described in [15]. All calculations were performed using the Gaussian 98 system of programs [16]. Throughout this paper, all inter-nuclear distances are in angstroms and all angles

Published online March 1, 2004

Address reprint requests to Dr. Y. Ren, Faculty of Chemistry, Sichuan University, P.O. Box 73, Chengdu 610064, P.R. China. E-mail: yiren57@hotmail.com



Scheme 1. Schematic potential energy profile for the $\text{Y}^- + \text{NMe}_2\text{X}$ non-identity gas-phase displacement reactions ($\text{Y}, \text{X} = \text{F}, \text{Cl}, \text{Br}, \text{and I}$).

are in degrees. Relative energies correspond to enthalpy changes at $0\text{K}[\Delta H(0\text{K})]$ in kJ/mol.

Results and Discussion

The gas-phase reaction energy profile for the concerted $\text{S}_{\text{N}}2$ reactions at nitrogen is described by an asymmetrical double-well curve for the non-identity reactions (Scheme 1). The reaction involves the initial formation of a reactant ion-molecule Complex **1**. This complex must then overcome the central barrier to reach an asymmetrical transition structure **2**. The latter then breaks down to give the product ion-molecule Complex **3**, which subsequently dissociates into the separate products. Analysis of the overall enthalpy changes indicates that the gas phase non-identity $\text{S}_{\text{N}}2$ reaction at nitrogen is exothermic only if the nucleophile is the lighter halide, which is same as the non-identity $\text{S}_{\text{N}}2$ reactions $\text{Y}^- + \text{CH}_3\text{X} \rightarrow \text{CH}_3\text{Y} + \text{X}^-$ ($\text{Y}, \text{X} = \text{F-I}$) [17]. The forward reactions are defined as exothermic in the following discussion. The key energetic quantities involved in reactions (eq 1), depicted in Scheme 1. Main geometries of all species involved in eq 1 are shown in Figure 1 and G2(+) energetics are listed in Tables 1 and 2.

Ion-Molecule Complexes

The calculated non-identity reactions of halides with halodimethylamine involve reactant and product ion-molecule complexes, **1** and **3** (Cs symmetry), which are characterized by two $\text{Y}^- \dots \text{HC}$ or $\text{CH} \dots \text{X}^-$ contacts (Figure 1), in contrast to the ones found in previous study of $\text{X}^- + \text{NH}_2\text{X}$ at the G2(+) level [8], where the corresponding symmetrically bridged forms are found to be transition structures for the migration of the X^- from one hydrogen to the other.

The G2(+) complexation enthalpies, $H^{\text{comp}}_{\text{XX}}$, for complexes $\text{X}^- \dots \text{Me}_2\text{NX}$ ($\text{Y}, \text{X} = \text{F-I}$) are smaller than $\text{H}^- \dots \text{HNHX}$ complexes (see Table 1), which are con-

sistent with the N-H bond being an more effective proton donor, leading to significant $\text{Y}^- \dots \text{HN}$ or $\text{NH} \dots \text{X}^-$ hydrogen bonding. The set of complexation enthalpies in Table 1 indicates that the complexation enthalpies depend primarily on the identity of nucleophile Y^- , and only to smaller extent on the identity of NMe_2X , and tend to decrease in the basicity order in the gas phase: $\text{F}^- > \text{Cl}^- > \text{Br}^- > \text{I}^-$, which is analogous to those found for $\text{S}_{\text{N}}2$ reactions at carbon [17] and oxygen [18]. Thus, the complexation enthalpies for $\text{Y} = \text{F}^-$ range between 91.5 and 101.6 kJ/mol, those for $\text{Y} = \text{Cl}^-$ range between 53.2 and 64.7 kJ/mol, those for $\text{Y} = \text{Br}^-$ range between 45.5 and 57.0 kJ/mol, while those for $\text{Y} = \text{I}^-$ range between 41.4 and 52.9 kJ/mol.

For a given NMe_2X , the complexation enthalpies show a good linear correlation with electronegativities of the halogen Y^- ($R^2 \approx 0.96$ for $\text{Y} = \text{F}, \text{Cl}, \text{Br}$, and I , respectively). This observation is in agreement with earlier finding that the G2(+) complexation enthalpies for $\text{Y}^- \dots \text{CH}_3\text{X}$ [17], $\text{X}^- \dots \text{HNHX}$ [8], and $\text{X}^- \dots \text{HOX}$ [19] ($\text{X} = \text{F-I}$) also decrease in the order $\text{F} > \text{Cl} > \text{Br} > \text{I}$. These correlations show that the interactions between halides Y^- ($\text{Y} = \text{F-I}$) and hydrogen atoms on methyl group will dominate the stabilization energies of complexes $\text{Y}^- \dots \text{Me}_2\text{NX}$.

The pattern of complexation energies for $\text{Y}^- \dots \text{Me}_2\text{NX}$ as a function of X shows the following ordering: $\text{NMe}_2\text{I} < \text{NMe}_2\text{Br} < \text{NMe}_2\text{F} < \text{NMe}_2\text{Cl}$. This fact suggests that both of the inductive effects of X (which would favor more electronegative atoms $\text{X} = \text{F}$ and Cl) and dimethylamino halide polarizability (which would favor larger atom $\text{X} = \text{Cl} \sim \text{I}$) will contribute to the stabilization of ion-molecule complex.

Transition State Structures and Barrier Heights

The TS structures at the G2(+) level of theory are found to have Cs symmetry for the non-identity reactions. The key parameters for describing the transition state are

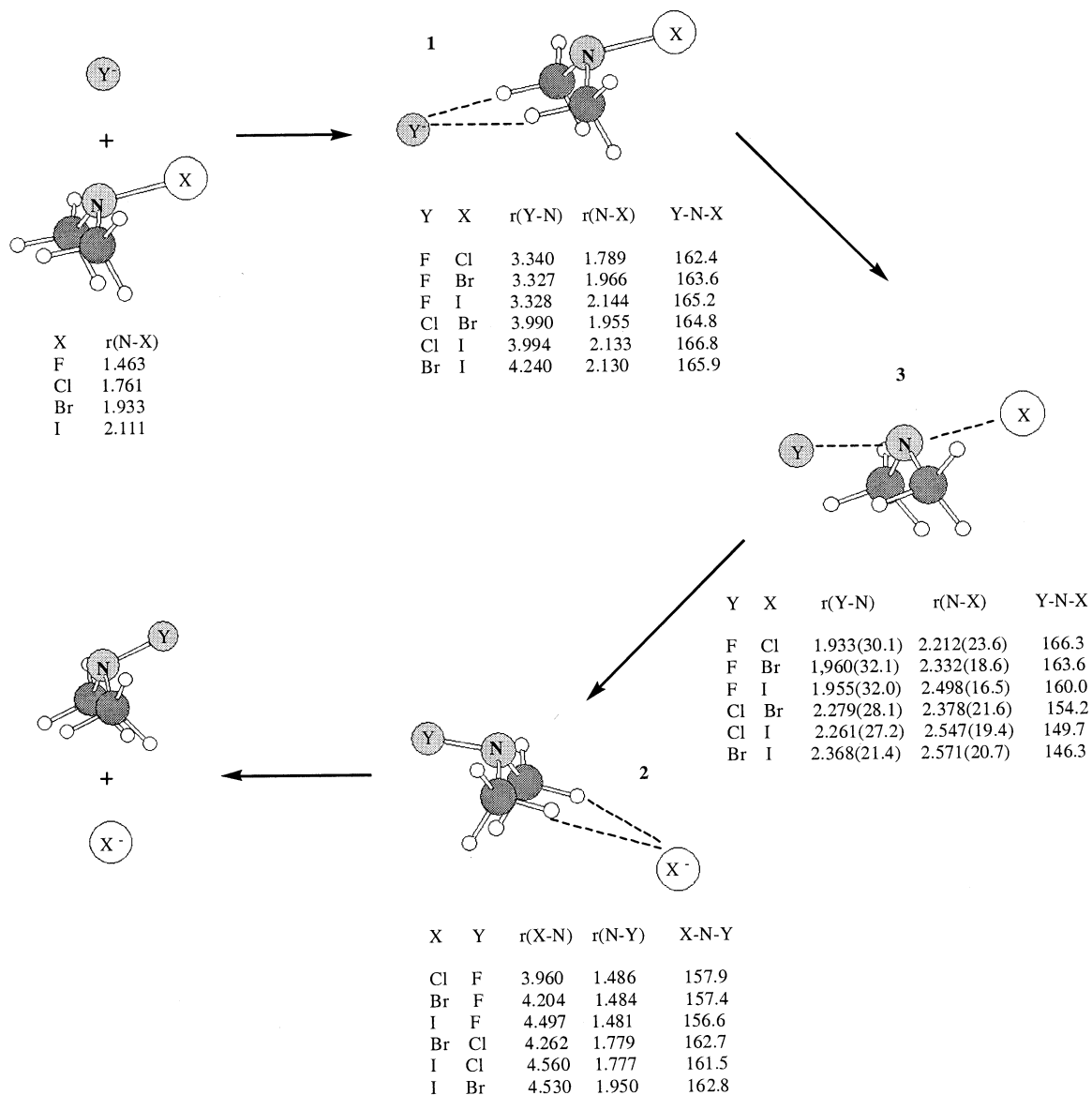


Figure 1. Main geometries of reactants, complexes, **1** and **3**, and transition structures **2**, in the reactions $\text{Y}^- + \text{NMe}_2\text{X}$ ($\text{Y} = \text{F}-\text{I}$; $\text{X} = \text{F}-\text{I}$) at the level of MP2(fc)/6-31 + G(d). The data in parentheses are the geometric looseness for the corresponding bonds calculated by eqs 2 and 3.

the distance between the halogen anion and the nitrogen atom. The main geometric feature in the transition structures is the elongations of the N-X and N-Y bonds relative to the ion-molecule complex. In a way similar to that proposed by Shaik et al. [20], we can readily define

the geometric looseness of N-X and N-Y bonds in the transition structures, $\% \text{N}-\text{X}^\#$ and $\% \text{N}-\text{Y}^\#$, and the composite transition structure looseness, $\% \text{L}^\#$:

$$\begin{aligned} \% \text{N}-\text{X}^\# &= 100[r^\#(\text{N}-\text{X}) - r^{\text{comp}} \\ &\quad (\text{N}-\text{X})]/r^{\text{comp}}(\text{N}-\text{X}) \end{aligned} \quad (2)$$

$$\begin{aligned} \% \text{N}-\text{Y}^\# &= 100[r^\#(\text{N}-\text{Y}) - r^{\text{comp}} \\ &\quad (\text{N}-\text{Y})]/r^{\text{comp}}(\text{N}-\text{Y}) \end{aligned} \quad (3)$$

$$\% \text{L}^\# = \% \text{N}-\text{X}^\# \% \text{N}-\text{Y}^\# \quad (4)$$

Table 1. G2(+) complexation enthalpies of the ion-molecule complexes **1** and **3**

	F^-	Cl^-	Br^-	I^-
NMe_2F	93.0 (114.0) ^a	56.3	48.6	44.4
NMe_2Cl	101.6	64.7 (67.8)	57.0	52.9
NMe_2Br	92.7	54.7	46.9 (58.4)	42.8
NMe_2I	91.5	53.2	45.5	41.4 (50.0)

^aValues in parentheses are the G2(+) complexation energies for $\text{X}^- + \text{NH}_2\text{X} \rightarrow \text{NH}_2\text{X} + \text{X}^-$ reactions ($\text{X} = \text{F}-\text{I}$) [8].

where $r^\#(\text{N}-\text{X})$ or $r^\#(\text{N}-\text{Y})$ and r^{comp} are the bond lengths in the transition structure **2** and the ion-mole-

Table 2. Central barrier heights (ΔH^{\ddagger}_{YX} and ΔH^{\ddagger}_{XY}), overall barrier heights (ΔH^b_{YX} and ΔH^b_{XY}), enthalpy differences between reactant and product ion-molecule complexes (ΔH), and overall reaction enthalpies (ΔH^{ovr}) for reactions $Y^- + NMe_2X \rightarrow X^- + NMe_2Y$ ($Y, X = F, Cl, Br, I$) at the G2(+) level in kJ/mol

Y, X	ΔH^{\ddagger}_{YX}	ΔH^b_{YX}	ΔH^b_{XY}	ΔH^{\ddagger}_{XY}	ΔH	ΔH^{ovr}
F, F	84.9 (58.2) ^a	-8.1 (55.8)				
Cl, Cl	96.4 (58.5)	31.7 (-9.3)				
Br, Br	82.8 (44.7)	35.9 (-13.7)				
I, I	72.6 (39.1)	31.3 (-10.8)				
F, Cl	75.7 73.5 ^b 11.9 13.4 ^c	-25.9 -24.3 (-55.5) -52.5 -42.4	55.6 57.1 75.0	111.9 109.6 114.3	-36.1 -102.4	-81.5 -127.5
F, Br	67.0 62.7 3.1 5.5	-25.7 -24.9 (-61.5) -65.8 -50.1	63.9 64.6 93.8	112.4 108.1 128.4	-45.4 -125.3	-89.5 -159.6
F, I	64.7 56.8 0.8 2.5	-26.8 -28.6 (-57.4) -68.9 -48.5	67.8 66.0 108.6	112.2 104.3 139.7	-47.5 -138.9	-94.6 -177.5
Cl, Br	85.0 84.5 39.5 39.6	30.3 29.8 (-17.2) -6.8 -5.9	38.3 37.9 25.3	95.3 94.9 64.3	-10.4 -24.8	-8.1 -32.1
Cl, I	81.1 78.2 32.0 31.6	27.9 25.1 (-12.5) -13.8 -12.1	41.0 38.2 36.1	93.9 91.1 70.6	-12.9 -38.6	-13.2 -49.9
Br, I	77.4 76.6 38.4 38.2	32.0 31.1 (-8.8) -2.3 -2.3	37.1 36.1 15.6	79.8 78.9 51.9	-2.4 -13.5	-5.1 -17.9

^aValues in parentheses are energetics of the $X^- + NH_2X \rightarrow X^- + NH_2Y$ reactions at G2 (+) level [8], in which the bold are calculated by eq. 7.

^bValues in bold are the calculated central barriers with eq. 6 and overall barriers with eq. 7.

^cValues in italic are the energetics of the $Y^- + CH_3X \rightarrow X^- + CH_3Y$ reactions at the G2 (+) level [17], in which the bold are calculated with eq. 6 and eq. 7.

cule complex (1 or 3), respectively.

As can be seen from the plot in Figure 2, a correlation of central barrier with %N-X or %N-Y is found, through of poorer quality (Figure 2, $R^2 = 0.911$), which suggests that the stretching of the cleaving bond is one of the major factors determining the central barrier heights (ΔH^{\ddagger}_{YX} and ΔH^{\ddagger}_{XY}). The other factor will be dimethylamino cation affinities (DMACA) for X^- [Dimethylamino cation affinities (DMACA) of halide anions are the energy changes for the reactions $NMe_2X \rightarrow NMe_2^+(^3B_1) + X^-$. Calculated G2(+) DMACA of halides are 823.1 kJ/mol($X = F$), 741.6 kJ/mol($X = Cl$), 733.5 kJ/mol($X = Br$) and 728.4 kJ/mol($X = I$), respectively.

We find the lowest singlet (1A_1) state of NMe_2^+ lies 12.5 kJ/mol above the 3B_1 ground state at the G2(+) level]; the calculations of G2(+) amino cation affinities (ACA) of halide anions can be seen in [8]. This is reasonable because the central barrier heights in the $Y^- + NMe_2X$ ($Y, X = F \sim I$) reactions should be mainly governed by the degree of bond cleavage (%N-X[#] or %N-Y[#]) and the energy changes for the reactions $NMe_2X \rightarrow NMe_2^+ + X^-$. If we observe correlation between the central barriers and the product of bond looseness and corresponding DMACA of halide anion, there is still a rough linear relationship ($R^2 = 0.902$). It is obvious that the former will be more important due to the smaller relative differences between the dimethylamino cation affinities for different X^- . It is worth noting that the better correlation between the central barriers and the bond looseness also existed in the non-identity S_N2 reactions at carbon ($R^2 = 0.973$) [17].

Furthermore, as observed for the non-identity methyl-transfer reactions [17], there is still a good correlation between forward central barriers, ΔH^{\ddagger}_{YX} , and the composite transition structure looseness, %L[#], for the reactions $Y^- + NMe_2X$ ($Y, X = Cl, Br$, and I) (Figure 3, $R^2 = 0.927$), but fails for the reactions $F^- + NMe_2X$ ($X = F-I$). This phenomena may be attributed to the significantly larger complexing energies for the complexes $F^- \dots Me_2NX$ than others, which will lead to the higher forward central barriers. Meanwhile, we note that the slope of linear regression for the correlation between ΔH^{\ddagger}_{YX} and %L[#] is positive in our paper, which is different from that found in the S_N2 reactions at carbon, where the slope is negative. This can be explained by stabilizing the transition state structures through the contribution of the triple-ion valence bond configuration, $Y^-CH_3X^-$ [17].

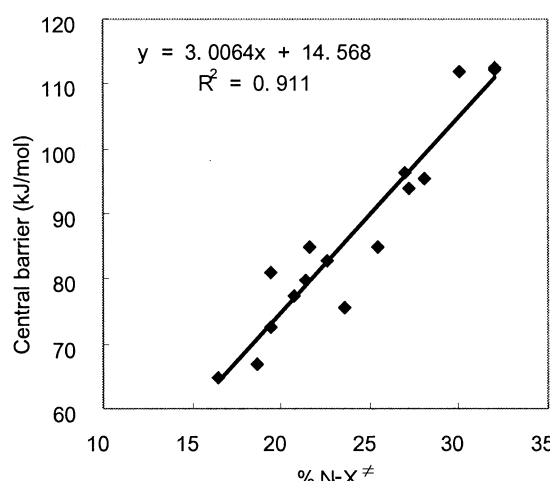


Figure 2. Plot of G2(+) central barriers ΔH^{\ddagger}_{YX} and ΔH^{\ddagger}_{XY} versus the geometric looseness of N-X and N-Y bonds of the transition structure 2 for the $Y^- + NMe_2X$ reactions ($Y, X = F-I$). ΔH^{\ddagger}_{YX} and ΔH^{\ddagger}_{XY} values are listed in Table 2. The geometric looseness of N-X and N-Y bonds are presented in Figure 1.

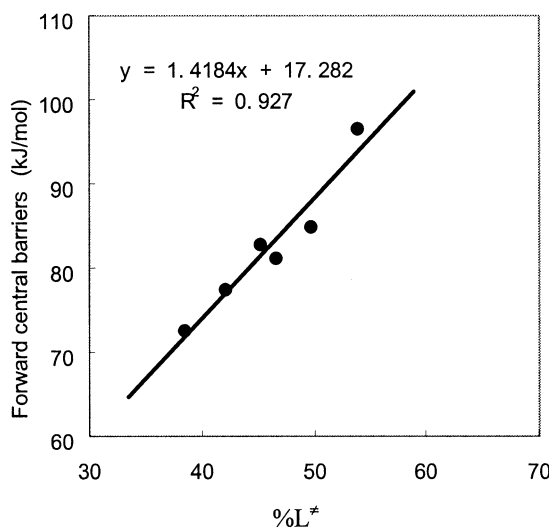


Figure 3. Plot of G2(+) forward central barrier, $\Delta H^\#_{YX}$, versus the composite transition structure looseness, $\%L^\#$, for the $Y^- + \text{NMe}_2\text{X}$ reactions ($Y, X = \text{Cl-I}$).

For the non-identity reactions at nitrogen (eq 1), the calculated central barriers at 0 K range from the 64.7 kJ/mol for the $\text{Br}^- + \text{NMe}_2\text{I}$ reaction up to 112.4 kJ/mol for the $\text{I}^- + \text{NMe}_2\text{F}$ reaction. According to the Marcus theory [10–12], in an exothermic reaction, a thermodynamic driving force will lower the transition state energy whereas endothermic driving force will induce higher activation energy. So, the forward central barrier heights $\Delta H^\#_{YX}$ should be lower than the intrinsic central barrier $\Delta H^\#_{0 YX}$ and the reverse central barrier heights $\Delta H^\#_{XY}$ should be higher than the intrinsic central barrier $\Delta H^\#_{0 XY}$. $\Delta H^\#_{0 YX}$ is estimated using the additivity postulate (eq 5). The G2(+) central barriers in Table 2 show that all of the reactions, including forward and reverse, are in agreement with Marcus theory.

$$\Delta H^\#_{0 YX} = 0.5[\Delta H^\#_{YY} + \Delta H^\#_{XX}] \quad (5)$$

The forward overall barriers ΔH^b_{YX} are found to be negative for $\text{F}^- + \text{NMe}_2\text{X}$ ($X = \text{F-I}$) reactions, which can be attributed to the significantly larger complexation energies for complexes $\text{F}^- \dots \text{Me}_2\text{NX}$ than others. In reverse direction, all of the overall barriers are positive.

Application of Marcus Theory

Marcus theory has been successfully applied to the interpretation of gas-phase S_N2 reactions at carbon [17] and oxygen [18]. It will be interesting to test the reliability of the Marcus theory for the S_N2 reactions at nitrogen. The Marcus equation

$$\Delta H^\#_{YX} = \Delta H^\#_{0 YX} + 0.5\Delta H + [(\Delta H)^2 / 16\Delta H^\#_{0 YX}] \quad (6)$$

relates the intrinsic barrier heights of a non-identity

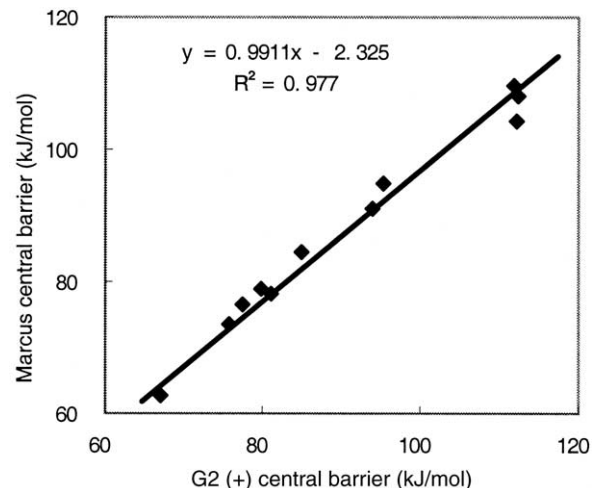


Figure 4. Plot of central barriers from eq 6 versus the same quantity obtained directly from the G2(+) theory for the reactions $Y^- + \text{NMe}_2\text{X}$ ($Y, X = \text{F-I}$). The values are listed in Table 2.

substitution reaction to the corresponding intrinsic barrier height in the absence of a thermodynamic driving force and the central enthalpy difference between product and reactant ion-molecule complexes **3** and **1**. We can see from Table 2 that the G2(+) central barrier heights are reproduced by Marcus theory within a few kJ/mol, the largest difference, mean signed error (MSE) and mean unsigned error (MUE) being 7.9, −3.1, 3.1 kJ/mol, respectively. A plot of Marcus central barriers by eq 6 versus the corresponding G2(+) data for the reactions $Y^- + \text{NMe}_2\text{X}$ ($Y, X = \text{F} \sim \text{I}$) gives a good linear correlation (Figure 4, $R^2 = 0.977$).

In order to apply the Marcus equation to the overall barriers, rather than the central barrier, Wolfe et al. [21] proposed the following modifications:

$$\begin{aligned} \Delta H^b_{YX} &= \Delta H^b_{0 YX} + 0.5\Delta H_{ovr} \\ &+ [(\Delta H_{ovr})^2 / 16\Delta H^\#_{0 YX}] \end{aligned} \quad (7)$$

$$\Delta H^b_{0 YX} = 0.5[\Delta H^b_{YY} + \Delta H^b_{XX}] \quad (8)$$

The eq 7 permits the predictions of the experimentally more accessible quantity from data of the corresponding identity reactions. The data in Table 2 illustrates the applicability of Wolfe equation to all of non-identity S_N2 reactions at nitrogen, the largest difference, MSE and MUE just being 2.8, −0.6, and 1.4 kJ/mol, respectively. There is a better correlation between the overall barriers obtained by Wolfe equation versus the corresponding G2(+) values (Figure 5, $R^2 = 0.998$) for eq 1 than corresponding correlation existed in non-identity S_N2 reactions at carbon ($R^2 = 0.990$) [17], that may be attributed to the smaller exothermicity for eq 1. The successful application of Marcus theory and its modification to the $Y^- + \text{NMe}_2\text{X}$ ($Y, X = \text{F} \sim \text{I}$) reactions imply that we can predict the enthalpies of transition structures for other non-identity S_N2 reactions at nitrogen

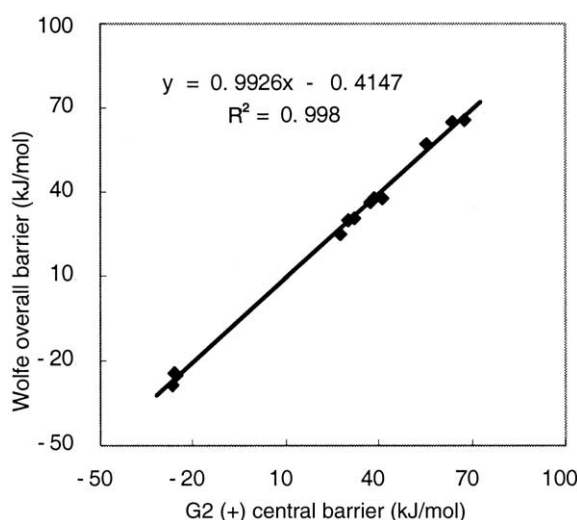


Figure 5. Plot of overall barriers from eq 7 versus the same quantity obtained directly from the G2(+) theory for the reactions $\text{Y}^- + \text{NMe}_2\text{X}$ ($\text{Y}, \text{X} = \text{F}-\text{I}$). The values are listed in Table 2.

using the central barriers of identity reactions if the non-identity reactions are not strongly exothermic.

Steric Effects

In the $\text{S}_{\text{N}}2$ reactions at carbon, increasing C-alkyl substitution has been shown to decrease the reaction rates, and to increase the intrinsic barriers [22]. This phenomenon is also observed for the nitrogen system. Comparison with $\text{Y}^- + \text{NH}_2\text{X}$ ($\text{Y}, \text{X} = \text{F}-\text{I}$) systems shows that the reactions $\text{Y}^- + \text{NMe}_2\text{X}$ ($\text{Y}, \text{X} = \text{F}-\text{I}$) will increase the overall barriers ($\Delta H_{\text{YX}}^{\text{b}}$) by ca. 37 kJ/mol (see Figure 6), due to the steric effects of two methyl groups in the transition state.

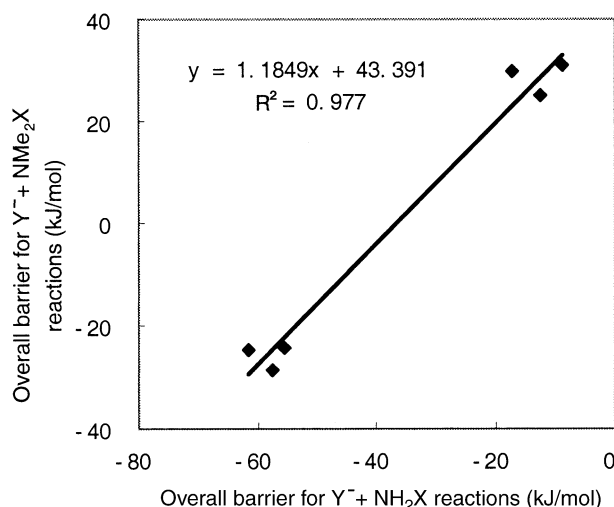


Figure 6. Plot of overall barriers for reactions $\text{Y}^- + \text{NMe}_2\text{X}$ ($\text{Y}, \text{X} = \text{F}-\text{I}$) versus overall barriers for reactions $\text{Y}^- + \text{NH}_2\text{X}$ ($\text{Y}, \text{X} = \text{F}-\text{I}$). All of the overall barriers are calculated by Wolfe equation (eq 7) and listed in Table 2.

Nucleophilicity and Leaving-Group Ability of Halides in Gas-Phase $\text{S}_{\text{N}}2$ Reactions at Nitrogen

The orders of nucleophilicity and the leaving-group ability are essential that describe for $\text{S}_{\text{N}}2$ reactions and will strongly affect the rate of the $\text{S}_{\text{N}}2$ reactions. Many properties have an influence on nucleophilicity, such as the medium of $\text{S}_{\text{N}}2$ reactions, the strength of its bond with central atom, and the electronegativity of the attacking atom. In the aliphatic $\text{S}_{\text{N}}2$ reactions, nucleophilicity of nucleophile in the solvent may be different from in the gas phase because of the solvation energy. The observed [23] and predicted [24, 25] reactivity sequences of nucleophiles in the gas-phase $\text{S}_{\text{N}}2$ reaction at carbon follow the order: $\text{F}^- > \text{Cl}^- > \text{Br}^- > \text{I}^-$, which will be reverse in the dipolar solvent, such as water and the alcohol. Here, we'll discuss the nucleophilicity and leaving-group ability of different halides in the gas-phase $\text{S}_{\text{N}}2$ reactions at nitrogen using our G2(+) energetics in Table 2.

Thermodynamic study. As shown in previous work [23], the exothermicity of the reactions of nucleophile with a single substrate reflects the thermodynamic affinity of the nucleophile. Following this idea, the exothermicity trend, in this work, is given by the sequences of the overall enthalpy change ΔH^{ovr} for the reaction as a function of nucleophile Y^- . It can be seen from Table 2 that no matter Y^- react any substrate, NMe_2F , NMe_2Cl , NMe_2Br , or NMe_2I , the exothermicity falls in following order: $\text{F}^- > \text{Cl}^- > \text{Br}^- > \text{I}^-$.

For example, ΔH^{ovr} for the $\text{Y}^- + \text{NMe}_2\text{I}$ ($\text{Y} = \text{F}, \text{Cl}, \text{Br}, \text{I}$) reactions are -94.6 , -8.1 , -5.1 , and 0.0 kJ/mol, respectively. This exothermicity can be clearly related to the nucleophilicity of Y^- , which follows the same trend.

If we fix the nucleophile Y^- and change the substrate NMe_2X going from $\text{X} = \text{F}$ to I , the exothermicity of the reactions increase in the same direction. This is certainly related to the leaving group ability, following in the order: $\text{F} < \text{Cl} < \text{Br} < \text{I}$.

Kinetic study. High-level computational study of Glukhovtsev et al. [8] for identity $\text{S}_{\text{N}}2$ reactions at nitrogen (eq 1) suggests that the more negative overall barrier heights, the more facile for the $\text{S}_{\text{N}}2$ reactions. The overall barriers for reactions $\text{Y}^- + \text{NMe}_2\text{F}$ ($\text{Y} = \text{F}, \text{Cl}, \text{Br}$, and I), as indicated in Table 2, show that the sequence given by $\Delta H_{\text{YX}}^{\text{b}}$ and $\Delta H_{\text{XY}}^{\text{b}}$ follows the following order, which is in agreement with the available experimental results [6]: $\text{F}^- (-8.1 \text{ kJ/mol}) < \text{Cl}^- (55.6 \text{ kJ/mol}) < \text{Br}^- (63.9 \text{ kJ/mol}) < \text{I}^- (67.8 \text{ kJ/mol})$.

With the other three substrates NMe_2Cl , NMe_2Br , and NMe_2I , the same orders are also obtained. These results are in good agreement with the exothermicity of reactions given in eq 1, showing the correlation between forward overall barriers and the overall reaction enthalpies ($R^2 = 0.992$), i.e., when the overall barriers decrease the exothermicity of the reactions increases. What is more, for a given nucleophile Y^- , the calculated overall

barriers decrease when going from X = F to I, which relates the leaving group ability increasing from F to I. In summary, the investigations of the kinetics and thermodynamics lead to the same conclusion.

Conclusions

Application of G2(+) theory to gas-phase non-identity exchange reactions of halide anions with halodimethylamine, Y⁻ + NMe₂X → NMe₂Y + X⁻ (Y, X = F-I), leads to the following conclusions:

1. The energy profile is described by an asymmetric double-well curve. The enthalpies of reactions are exothermic only when the nucleophile is the lighter halide, in agreement with those in non-identity substitution reactions at carbon.
2. The complexation energies for complexes depend on the identity of nucleophile and are found to correlate well with the electronegativities of the nucleophile.
3. The forward central barrier heights, ΔH_{YX}[#], are lower than the intrinsic central barrier ΔH_{0 YX}[#] and the lowering is attributed to the effect of forward reaction exothermicity which ranges from -94.6 kJ/mol for F⁻ + NMe₂I to -5.1 kJ/mol for Br⁻ + NMe₂I.
4. The overall barriers are all negative for the forward reactions involving the fluorine (ΔH^b_{FX}) and positive for other reactions, which suggest that the reactions F⁻ + NMe₂X → NMe₂F + X⁻ (X = F-I) are more facile than others.
5. The set of non-identity reactions Y⁻ + NMe₂X (Y, X = F, Cl, Br, I) obeys the Marcus equation. The central barriers estimated by Marcus equation are close to the directly calculated central barrier and a plot of the two data sets gives a good correlation ($R^2 = 0.977$). A modified Marcus equation used to estimate the overall barriers for reactions Y⁻ + NMe₂X (Y, X = F, Cl, Br, I) is found to be more reliable ($R^2 = 0.998$).
6. Central barriers, ΔH_{YX}[#] and ΔH_{XY}[#], exhibit reasonable linear relationship with the geometric looseness of N-X and N-Y bonds in the transition structures. There is a good correlation between forward overall barriers and overall enthalpy changes.
7. Combining the G2(+) results of kinetic and thermodynamic investigations, we predict that the nucleophilicity for halide anions in the reactions (eq 1) follow the order: F⁻ > Cl⁻ > Br⁻ > I⁻, and the leaving-group ability is reverse: F < Cl < Br < I.

Acknowledgments

YR is thankful for the support from the Barbara and Kort Sino-Israel Post-Doctoral Fellowship Program and the Scientific Research Foundation for the Returned Chinese Scholars of State Education Ministry and Sichuan University. HJZ thanks the support of Bairenjihua Fund from CAS and Fund (NSFC#20242012).

References

1. Erdik, E.; Ay, M. Electrophilic Amination of Carbanions. *Chem. Rev.* 1989, 89, 1947–1980 (and references cited therein).
2. Ulbrich, R.; Famulok, M.; Bosold, F.; Boche, G. S_N2 at Nitrogen: The Reaction of N-(4-Cyanophenyl)-O-Diphenylphosphinoylhydroxylamine with N-Methylaniline. A Model for the Reactions of Ultimate Carcinogens of Aromatic Amines with (Bio)nucleophiles. *Tetrahedron Lett.* 1990, 31, 1689–1692.
3. Helmick, J. S.; Martin, K. A.; Heinrich, J. L.; Novak, M. Mechanism of the Reaction of Carbon and Nitrogen Nucleophiles with the Model Carcinogens O-Pivaloyl-N-Arylhydroxylamines: Competing S_N2 Substitution and S_N1 Solvolysis. *J. Am. Chem. Soc.* 1991, 113, 3459–3466.
4. Sheradsky, T.; Yusupova, L. Intramolecular Nucleophilic Substitution on Nitrogen. A New Heterocyclic Synthesis. *Tetrahedron Lett.* 1995, 36, 7701–7704.
5. Beak, P.; Li, J. The Endocyclic Restriction Test: Experimental Evaluation of Transition-Structure Geometry for a Nucleophilic Displacement at Neutral Nitrogen. *J. Am. Chem. Soc.* 1991, 113, 2796–2797.
6. Gareyev, R.; Kato, S.; Bierbaum, V. M. Gas Phase Reactions of NH₂Cl with Anionic Nucleophiles: Nucleophilic Substitution at Neutral Nitrogen. *J. Am. Soc. Mass Spectrom.* 2001, 12, 139–143.
7. Bühl, M.; Schaefer, H. F. S., III. S_N2 Reactions at Neutral Nitrogen: Transition State Geometries and Intrinsic Barriers. *J. Am. Chem. Soc.* 1993, 115, 9143–9147.
8. Glukhovtsev, M. N.; Pross, A.; Radom, L. Gas Phase Identity S_N2 Reactions of Halides Ions at Neutral Nitrogen: A High-Level Computational Study. *J. Am. Chem. Soc.* 1995, 117, 9012–9018.
9. Ren, Y.; Basch, H.; Hoz, S. The Periodic Table and the Intrinsic Barrier in S_N2 Reactions. *J. Org. Chem.* 2002, 67, 5891–5895.
10. Marcus, R. A. Chemical and Electrochemical Electron-Transfer Theory. *Annu. Rev. Phys. Chem.* 1964, 15, 155–196.
11. Marcus, R. A. Theoretical Relations Among Rate Constants, Barriers, and Brønsted Slopes of Chemical Reactions. *J. Phys. Chem.* 1968, 72, 891–899.
12. Albery, W. J. The Application of the Marcus Relation to Reactions in Solution. *Annu. Rev. Phys. Chem.* 1980, 31, 227–263.
13. Curtiss, L. A.; Raghavachari, K.; Trucks, G. W.; Pople, J. A. Gaussian-2 Theory for Molecular Energies of First- and Second-Row Compounds. *J. Chem. Phys.* 1991, 94, 7221–7230.
14. Wadt, W. R.; Hay, P. J. Ab Initio Effective Core Potentials for Molecular Calculations. Potentials for Main Group Elements Na to Bi. *J. Chem. Phys.* 1985, 82, 284–298.
15. Glukhovtsev, M. N.; Pross, A.; Radom, L. Gas Phase Identity S_N2 Reactions of Halides Anions with Methyl Halides: A High-Level Computational Study. *J. Am. Chem. Soc.* 1995, 117, 2024–2032.
16. Frisch, M. J.; Trucks, G. W.; Schlegel, H. B.; Scuseria, G. E.; Robb, M. A.; Cheeseman, J. R.; Zakrzewski, V. G.; Montgomery, J. A.; Stratmann, R. E., Jr.; Burant, J. C.; Dapprich, S.; Millam, J. M.; Daniels, A. D.; Kudin, K. N.; Strain, M. C.; Farkas, O.; Tomasi, J.; Barone, V.; Cossi, M.; Cammi, R.; Mennucci, B.; Pomelli, C.; Adamo, C.; Clifford, S.; Ochterski, J.; Petersson, G. A.; Ayala, P. Y.; Cui, Q.; Morokuma, K.; Malick, D. K.; Rabuck, A. D.; Raghavachari, K.; Foresman, J. B.; Ciosowski, J.; Ortiz, J. V.; Baboul, A. G.; Stefanov, B. B.; Liu, G.; Liashenko, A.; Piskorz, P.; Komaromi, I.; Gomperts, R.; Martin, R. L.; Fox, D. J.; Keith, T.; Al-Laham, M. A.; Peng, C. Y.; Nanayakkara, A.; Gonzalez, C.; Challacombe, M.; Gill, P. M. W.; Johnson, B.; Chen, W.; Wong, M. W.; Andres, J. L.;

- Head-Gordon, M.; Replogle, E. S.; Pople, J. A. *Gaussian 98, Revision A.7*; Gaussian, Inc.: Pittsburgh, PA, 1998.
17. Glukhovtsev, M. N.; Pross, A.; Radom, L. Gas Phase Non-Identity S_N2 Reactions of Halides Anions with Methyl Halides: A High-Level Computational Study. *J. Am. Chem. Soc.* **1996**, *118*, 6273–6284.
18. Ren, Y.; Wolk, J. L.; Hoz, S. Hybrid DFT Study on the Gas-Phase S_N2 Reactions at Neutral Oxygen. *Int. J. Mass. Spectrom.* **2003**, *225*, 167–176.
19. Ren, Y.; Wolk, J. L.; Hoz, S. A G2(+) Level Investigation of the Gas-Phase Identity Nucleophilic Substitution at Neutral Oxygen. *Int. J. Mass Spectrom.* **2002**, *220*, 1–10.
20. Shaik, S. S.; Schlegel, H. B.; Wolfe, S. Theoretical Aspects of Physical Organic Chemistry. The S_N2 Mechanism; Wiley: New York, 1992, pp 181–188.
21. Wolfe, S.; Mitchell, D. J.; Schlegel, H. B. Theoretical Studies of S_N2 transition states. 2. Intrinsic Barriers, Rate-Equilibrium Relationships and the Marcus Equation. *J. Am. Chem. Soc.* **1981**, *103*, 7694–7696.
22. Jensen, F. A Theoretical Study of Steric Effects in S_N2 Reactions. *Chem. Phys. Lett.* **1992**, *196*, 368–376.
23. Olmstead, W. N.; Brauman, J. I. Gas-Phase Nucleophilic Displacement Reactions. *J. Am. Chem. Soc.* **1977**, *99*, 4219–4228.
24. Shaik, S. S.; Hiberty, P. C. VB Mixing and Curve Crossing Diagrams in Chemical reactivity and Bonding. *Adv. Quantum Chem.* **1995**, *26*, 99–163.
25. Safi, B.; Choho, K.; Geerlings, P. Quantum Chemical Study of the Thermodynamic and Kinetic Aspects of the S_N2 Reaction in Gas Phase and Solution Using a DFT Interpretation. *J. Phys. Chem. A* **2001**, *105*, 591–601.